EAGE

NFR02

Diffraction imaging of the Wisting Discovery

T.J. Moser[3], L.M. Moskvil[2], E. Angerer[1], W. Kobusinski[5], M. Pelissier[4], J. Orosz[1]

[1] OMV Exploration & Production GmbH; [2] OMV (Norge) AS; [3] MGS; [4] IGS; [5] Geofizyka Torun SA

Summary

Seismic diffraction imaging (DI) is applied to the Barents Sea Wisting field, using the velocity and reflection dip fields obtained from a legacy PSDM. The objective is to image steeply dipping faults. The fault definition obtained from the DI is compared to the legacy PSDM and also to a high resolution P-cable survey. The improved resolution and detectability of the fault systems by DI offer a significant added value for interpretation of the legacy PSDM as well as the P-cable.

Introduction

This paper details the seismic diffraction imaging of the Wisting discovery located in the Barents Sea Hoop-Maud basin, at a water depth of 400 m and a reservoir depth of approximately 250m below seabed. This field features a wide range of challenges and as such has attracted the application leading technologies and is known in the industry as a “seismic laboratory” (Veire et al. 2016). This comprise a wide range of data; such as 3D seismic data, extensive 2D site survey data, an extensive well log suite and 3D CSEM data. To be able to further mature the Wisting discovery towards field development, improved ability to perform detailed reservoir characterization and a better understanding of the reservoir architecture is considered crucial. To achieve this, OMV and the partners acquired a new ultra-high resolution seismic dataset (P-cable) in 2016 (Garden et al. 2017 and Moskvil et al. 2018). The discovery is heavily compartmentalized by complementary sets of steeply dipping NW-SE and NE-SW trending faults. The objective of the DI is to extend the seismic resolution and detectability limits of the faulting at reservoir level and the extension of these faults into the overburden. The DI was conducted on the conventional data and using the higher fault definition of the broadband P-cable data as an important reference for validation.

In comparison to conventional PSDM, the diffraction imaging provides significant additional resolution of sub-wavelength scale features as well as a fundamental advantage in terms of illumination for steeply dipping features (Moser and Howard 2008). In our workflow, the diffraction imaging is carefully calibrated to interpretation objectives – we refer to this as Customization to Interpretation (CTI). At all stages of the imaging workflow, the legacy PSDM and broadband data and intermediate DI results are quality controlled and carefully calibrated in the interpretation environment. The interpretation workflows for DI are fundamentally different from those of conventional seismic attributes derived from post-migration post-stack PSDM data. This is because the diffraction image is a wavefield, as opposed to an attribute, and provides a unique way of Fresnel zone sampling of subsurface features of various scales.

Imaging Workflow

The DI workflow consists of the following steps: 1. Reflector dip extraction from the legacy PSDM by least squares dip estimation. 2. PSDM with partial migration output sorted into specularity gathers. This step involves specific choices in order to ensure an optimal preservation of diffraction content. 3. Tapering and stacking the specularity gathers. The specularity taper design involves a careful sampling of the Fresnel zone and selecting which part of the Fresnel zone should enter into the diffraction image. This process is closely calibrated by the customization to interpretation (CTI). In this paper, DI at $\alpha°$ stands for DI tapered at angle $\alpha°$, full specularity stack refers to the untapered stack which is equivalent to normal PSDM (details and further references in Pelissier et al., 2017).

Results

The DI has provided an uplift in the overburden and at the reservoir level. This includes iceberg plough marks and polygonal faulting in the overburden and extensive faulting at the reservoir level. At a depth of around 500m TVDSS we encounter a very complex system of polygonal faulting (as detailed by Ostanin et al., 2012). Whereas this is clearly imaged by the P-cable data, the signature of this faulting is absent on the legacy PSDM as shown in Figure

1. The specularity tapers applied to the legacy data bring out details that are comparable to the P-cable albeit with a lesser inherent resolution. The uplift in resolution is due to two considerations: the re-parameterization with respect to specularity as opposed to offset, and the calibrated suppression of reflectivity. The full specularity stack primarily includes the re-parameterization and shows the polygonal faulting combined with reflectivity. This reflectivity is then suppressed in the DI taper, which also shows improved definition of the faulting.

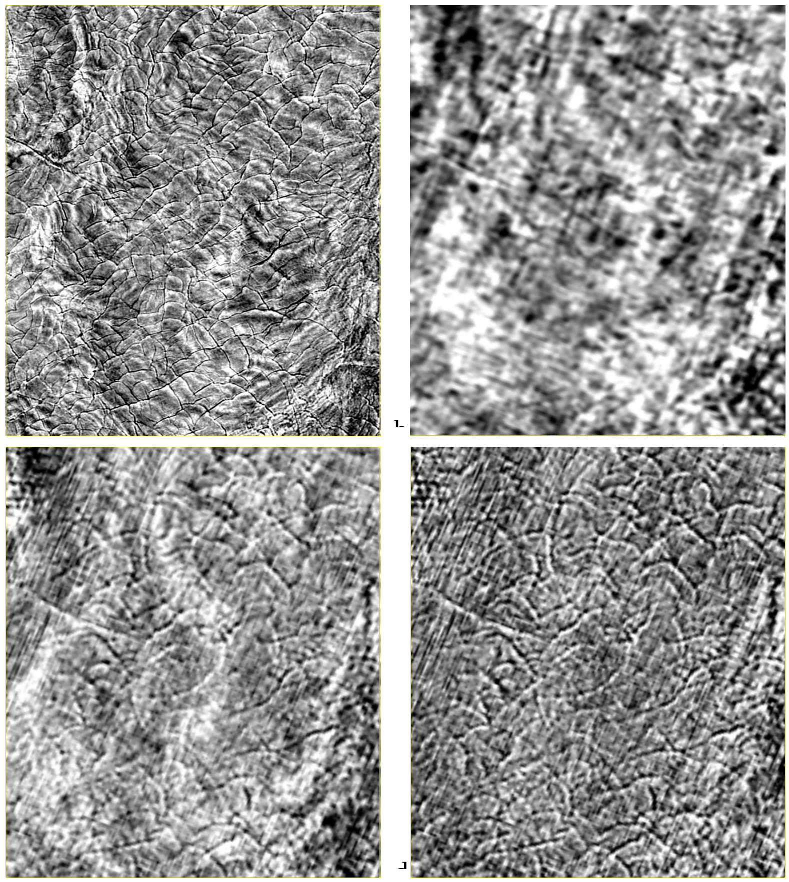

Figure 1 *Polygonal faults at depth 508 m TVDSS. a) P-cable PSDM, b) legacy PSDM, c) full specularity stack, d) DI at 16°.*

The legacy and P-cable PSDM are shown in Figure 2 along with the DI at 32° as both a semi-transparent overlay and as diffraction fault likelihood (DFL) derived from the same DI amplitudes. DFL is a thinned fault likelihood similar to that described by Hale (2013). However, instead of being derived from semblance, this is derived from the diffraction amplitude peak or trough distribution (trough amplitude in this case). The semi-transparent overlay clearly shows the steeply dipping faults as well as their extension into the overburden. This provides a distinct uplift in fault definition for both the legacy and P-cable. The DFL has correctly placed many of the fault planes and has the advantage of being derived directly from the diffracted wavefield as opposed to a post-stack post-migration attribute.

The DFL consists of three properties: likelihood, strike and dip. These can be filtered to pick up specified trends and remove outliers; in Figure 2 we display the raw DFL. The same applies to the depth slices in Figure 3 where DFL is overlain on the semblance of the P-cable and on the legacy PSDM amplitude. Essentially, the DFL captures all of the main features shown on the P-cable semblance, which has inherently higher resolution than the semblance of the legacy PSDM. Some acquisition footprint is also picked up by the DFL that needs to be discarded. In places, the DFL derived from DI of the legacy data adds to the fault detail provided in depth slices by P-cable semblance.

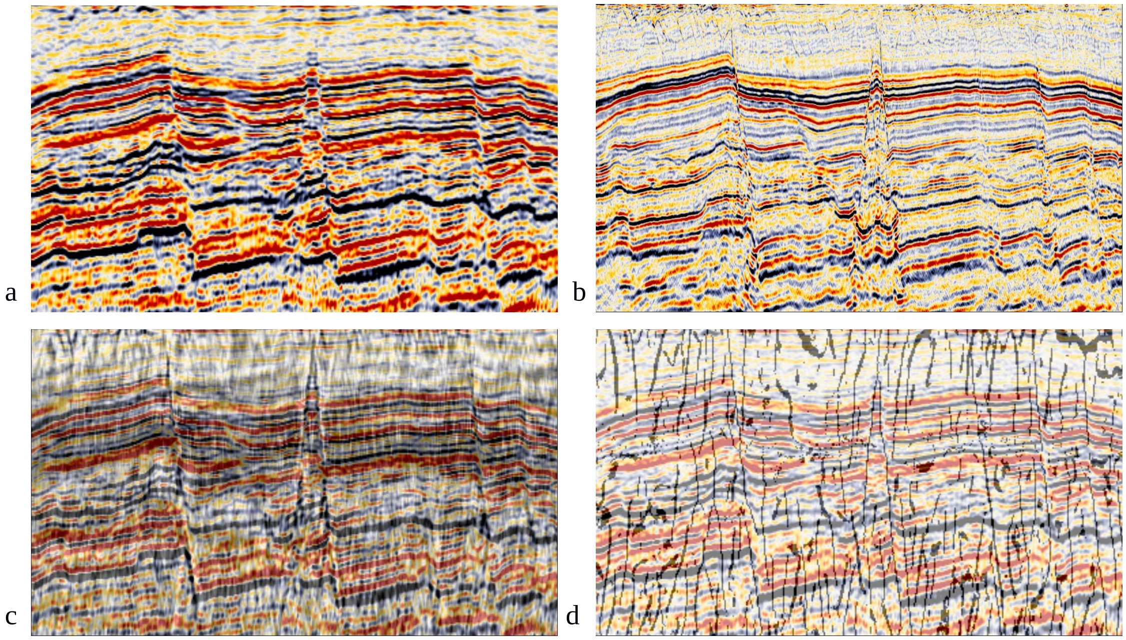

Figure 2 *Section over reservoir target a) Legacy PSDM , b) P-cable PSDM, c) DI at 32° overlain on legacy PSDM , d) Diffraction Fault Likelihood (DFL) overlain on legacy PSDM.*

Conclusions and Recommendations

DI derived from the Wisting field legacy data provides a significant uplift in fault definition not only for the legacy data. A polygonal fault system in the overburden, that is visible in P-cable but not the legacy PSDM, is nevertheless brought out by the diffraction imaging of the legacy data. Iceberg plough marks are also uncovered by the DI.

The fault definition at reservoir level is clearly improved by the DI bringing it to a level comparable with P-cable PSDM. The DI also serves to detail the upward extension of faulting from the reservoir level into the overburden. The quality of the fault imaging is sufficient to support the derivation of diffraction fault likelihood which compares very favorably with the semblance derived from the P-cable.

The availability of the P-cable data in the Wisting "seismic laboratory" provides an outstanding opportunity to validate the DI results and demonstrate its remarkable potential for improved detectability and resolution. This gives us confidence to push for DI not only in the presence of good quality seismic but also in challenging settings with complex geology that often results in lower quality refection seismic images.

Acknowledgements

We would like to acknowledge Emerson /Paradigm for their contribution in the continuous development of the FAZ depth imaging technology and the partners in license PL537 Equinor, Idemitsu, and Petoro.

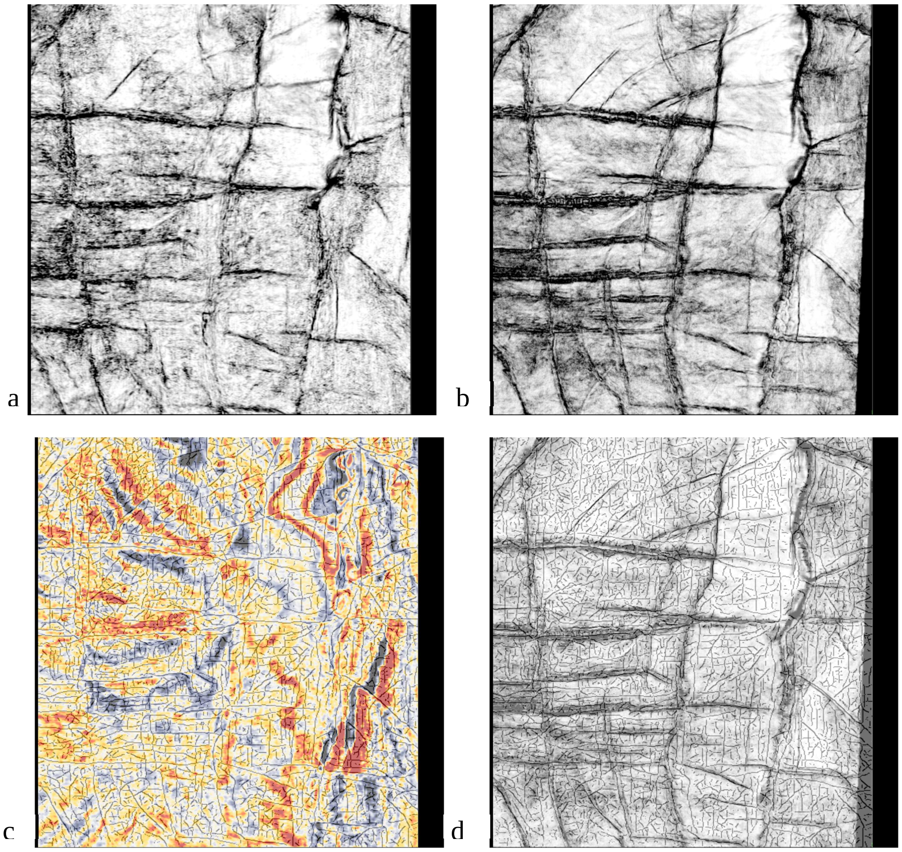

Figure 3 *Depth slice at 750 m TVDSS. a) Semblance from legacy PSDM, b) Semblance from P-cable PSDM , c) Legacy PSDM with DFL overlain. d) Semblance from P-cable PSDM with DFL overlain*

References

Garden M., Michot O., Terenzoni M., Veire H.H., Granli J.R., Moskvil L.M. and Krathus-Larsen K.I. 2017. Resolution, Resolution, Resolution - An Ultra-high Resolution Seismic Case Study from the Barents Sea, 79*th EAGE Conference and Exhibition, Paris.*

Hale D. 2013. Methods to compute fault images, extract fault surfaces, and estimate fault throws from 3D seismic images. *Geophysics*, **78(2)**, O33–O43.

Moser T.J. and Howard C.B. 2008. Diffraction imaging in depth. *Geophysical Prospecting*, **56**, 627-641.

Moskvil L.M, Granli J.R, Veire H.H, Larsen K. K, Stueland E, Michot O, Garden M "Keynote: High Resolution Seismic Acquisition at Wisting", EAGE marine Acquisition Workshop, Oslo, Norway, 2018

Ostanin, I., Anka, Z., di Primio, R. and Bernal, A. 2012. Identification of a large Upper Cretaceous Polygonal Fault network in the Hammerfest Basin: Implications on the reactivation of regional faults and gas leakage dynamics, SW Barents Sea. *Marine Geology*, *332-334*, 109—125.

Pelissier M., Moser T.J., Yu C., Lang J., Sturzu I. and Popovici A.M. 2017. Interpretation value of diffractions and sub-specular reflections – applications on the Zhao Dong field, *First Break*, **35**, 61-68.

Veire H., Granli J.R., Berger P., Lewis O., Hohner M., Kvist-Lassen T., Smith P. and Stuberg L. 2016. The Wisting Discovery - Integrating Acoustic Measurements at Different Scales, *78th EAGE Conference and Exhibition, Vienna.*